

# An INDO-CI Method in $\pi$ -Approximation for the Calculation of Transition Metal Complexes with Organic Ligands—Application to Iron(II)-trisdiimine Complexes

Christiane Jung\*, Otto Ristau

Central Institute of Molecular Biology of the Academy of Sciences of the GDR, Department of Hemecatalysis, 1115 Berlin, German Democratic Republic

Christoph Jung

Faculty of Chemistry of the Humboldt-University Berlin, German Democratic Republic

An INDO-CI method in  $\pi$ -approximation extended for transition metal complexes with organic ligands is presented. The  $\sigma$ -polarization in the complex is estimated using a two-dimensional EHT calculation and considered in the  $\pi$ -calculation by means of the diagonal Fock matrix elements. The method is tested for four trisdiimine iron(II) complexes. In agreement with the experimental absorption spectra the calculations show that diimine complexes with non-heterocyclicly bound nitrogen atoms exhibit a large red-shift of the characteristic charge-transfer transition increasing the number of aromatic rings. Contrarily, for diimine complexes with heterocyclicly bound nitrogen atoms no shift of the charge-transfer transition was obtained.

**Key words:** Closed-shell INDO-CI method—Trisdiimine iron(II) complexes.

## 1. Introduction

The bands of electronic absorption spectra of organic metal complexes originate from different types of electronic transitions: intra-ligand transitions, charge-transfer transitions and d–d transitions. d–d transitions are Laporte-forbidden

\* To whom correspondence should be addressed.

[1]. Only small transition probabilities can be induced by perturbations of the high symmetry of the complexes. The intra-ligand transitions are predominantly influenced by the interaction with charge-transfer transitions. For example such an interaction is responsible for the change of the energies and intensities of the electronic transitions of iron porphyrin complexes if the nature of the axial ligands is changed. To investigate the influence of the axial ligands to the absorption spectra of the biologically important hemoproteins which contain an iron porphyrin complex as prosthetic group quantum chemical calculations of the electronic transitions are carried out. Assuming that the absorption bands of the porphyrin complexes predominantly originate from  $\pi \rightarrow \pi^*$  transitions of the porphyrin ligand itself a  $\pi$ -electron procedure should be suitable for such calculations. Three versions of a  $\pi$ -electron procedure for metal complexes exist in the literature until now (Hanazaki et al. [2], Sanders [3] and Roos [4]).

Although these procedures show some inconsistencies or disadvantages (see below) concerning the influence of the  $\sigma$ -system on the  $\pi$ -system, no further progress for a qualification of these methods is detectable in the literature since about eight years (neglecting the extension of Sanders' method to open-shell complexes [5]). The quantum chemical method presented here is an INDO-CI method in the  $\pi$ -electron approximation with PPP-like parametrization. To avoid the disadvantages of the mentioned three methods [2, 3, 4] a procedure for the consideration of the  $\sigma$ -system was developed.

This paper gives the theoretical background of the method and its test to simple iron complexes – the trisdiimine iron(II) complexes.

## 2. Theoretical Method

Before the details of the proposed  $\pi$ -INDO-CI method are presented the already mentioned three  $\pi$ -electron procedures for metal complexes will be briefly reviewed. (i) The method from Hanazaki et al. [2] is a PPP-MIM method and was applied to iron(II) trisdiimine complexes. The SCF calculation was carried out for the isolated diimine ligands considering the iron by means of a variable point charge in the electrostatic term of the diagonal Fock matrix element. For the calculation of the excited states a MIM matrix with the ground state configuration, the local ligand excited configurations and charge-transfer configurations were formed. The disadvantage of this method is the loss of the relationship between ligand- $\sigma$ -donation and iron- $\pi$ -backdonation caused by the neglect of the resonance integrals between the iron and the ligands in the SCF calculation. (ii) Sanders' method [3] is an INDO procedure in  $\pi$ -electron approximation with explicit consideration of the metal. The gauge parameter is the charge of the metal. This method neglects the charge on the ligand atoms bound to the metal which originates from the ligand- $\sigma$ -donation to the metal. Therefore, the total charge of the complex is not maintained in the calculations by variation of the metal charge. This method was also applied to iron(II) trisdiimine complexes. (iii) The PEEL method from Roos [4] is also an INDO procedure which considers the  $\pi$ -orbitals of the ligands, the lone-pair orbital of the ligand atoms

bound to the metal and the valence orbitals of the metal. The SCF cycle is repeated up to the selfconsistency of the metal charge. This method was used for the interpretation of the absorption spectra and Mößbauer data of iron(II)-trisdiimine complexes [6]. As shown below the differences between the absorption spectra of different diimine complexes were incorrectly calculated by this method.

The method presented here uses the “coupled  $\pi$ -orbital model” meaning that the  $d\pi$  orbitals ( $d_{xz}$ ,  $d_{yz}$ ,  $d_{xy}$ ) of the metal couple two ligand  $\pi$ -systems perpendicular to each other. According to the method by Saunders [3] the  $\sigma/\pi$  separation is consequently carried out, i.e. the symmetry-allowed interactions between the  $\sigma$  and the  $\pi$  orbitals are neglected. IEHT calculations of metal porphyrin complexes [7] have shown that these interactions are weak comparing with  $\pi-d\pi$  interactions. An estimation of the  $\sigma$ -core-charge distribution between the metal and the ligands precedes the  $\pi$ -electron calculation. The  $k_\sigma$  factor of the EHT-resonance integral between the ligand lone pair orbitals and the metal  $d^2sp^3$  hybrid orbitals necessary for this estimation is the gauge parameter of the method. The method is developed according to the INDO approximation. The CI calculations for the excited states are carried out with singly excited configurations.

### 2.1. SCF Equations and Their Parametrization

The SCF calculations are performed using the Fock matrix elements for closed-shell systems according to the INDO approximation [8] given in Eqs. (1–3):

$$F_{\mu\mu}^A = H_{\mu\mu}^A + \frac{1}{2}P_{\mu\mu}\gamma_{\mu\mu} + \sum_{\nu \neq \mu} P_{\nu\nu}(\gamma_{\mu\nu} - \frac{1}{2}K_{\mu\nu}) + \sum_{B \neq A} \sum_{\rho} P_{\rho\rho}\gamma_{\mu\rho} \quad (1)$$

$$F_{\mu\nu}^A = -\frac{1}{2}P_{\mu\nu}\gamma_{\mu\nu} + \frac{3}{2}P_{\mu\nu}K_{\mu\nu} \quad (2)$$

$$F_{\mu\rho}^{A,B} = \beta_{\mu\rho} - \frac{1}{2}P_{\mu\rho}\gamma_{\mu\rho} \quad (3)$$

$A$  and  $B$  refer to the atoms.  $\mu$ ,  $\nu$  and  $\rho$  indicate the  $\pi$ -orbitals.  $H$ ,  $P$ ,  $\beta_{\mu\rho}$ ,  $\gamma_{\mu\nu}$  and  $K_{\mu\nu}$  are the core matrix, the charge density-bond order matrix, the resonance integral, the two-electron Coulomb integral and the one-center exchange integral, respectively.

### 2.2. One-Center-One-Electron Integral $H_{\mu\mu}^A$

The main problem of the parametrization concerns to the  $H_{\mu\mu}^A$  integrals in the Fock matrix element  $F_{\mu\mu}^A$  (Eq. 1).  $H_{\mu\mu}^A$  is usually written as shown in Eq. (4).

$$H_{\mu\mu}^A = U_{\mu\mu}^A - \sum_{B \neq A} V_{\mu B} \quad (4)$$

$U_{\mu\mu}^A$  represents the pure one-atomic core integral (Eq. (5)).

$$U_{\mu\mu}^A = (\mu|T(1) - Z_A/r_{1A}|\mu) + \sum_s^A (2\gamma_{\mu s} - K_{\mu s}) \quad (5)$$

$V_{\mu B}$  is a two-center integral.

$$V_{\mu B} = (\mu|Z_B/r_{1B}|\mu) - \sum_r^B (2\gamma_{\mu r} - K_{\mu r}) \quad (6)$$

$T(1)$ ,  $Z_{A(B)}$  and  $r_{1A(B)}$  are the operator of the kinetic energy, the nucleus charge of  $A(B)$  and the distance between the electron 1 and the atom  $A(B)$ , respectively. The indices  $s$  and  $r$  refer to the  $\sigma$ -orbitals.

Eq. (5) and (6) correspond to the case that the  $\sigma$ -core charges of  $A$  and  $B$  are equal with their number of  $\pi$ -electrons. In molecules with heteroatoms and especially in metal complexes, however, a large shift of charges exists in the  $\sigma$ -system. Assuming that the partial core-charges  $\delta_A$  and  $\delta_B$  are localized only in one  $\sigma$ -orbital  $\sigma$  and  $\sigma'$ , respectively (for example the lone-pair orbital of ligands and the empty  $d\sigma$  orbitals of the metal) than the one-electron integrals for the partially charged atoms  $A$  and  $B$  are corrected by a term  $\delta_{A(B)}\gamma_{\mu\sigma(\sigma')}$ .

$$\begin{aligned} U_{\mu\mu}^{\delta_A} &= U_{\mu\mu}^A - \delta_A \gamma_{\mu\sigma} \\ V_{\mu B}^{\delta_B} &= V_{\mu B} + \delta_B \gamma_{\mu\sigma'} \end{aligned} \quad (7)$$

$U_{\mu\mu}^A$  is usually expressed by the valence state ionization potential  $I_{\mu}^A$  of the neutral atom  $A$  and the coulomb interaction with other electrons.  $I_{\mu}^A$  results from the energy difference between the  $\pi$ -cation and the neutral atom ( $E^+(\mu) - E^0$ ). For the charge-corrected one-center integral  $U_{\mu\mu}^{\delta_A}$  the following equation results from Eq. (5).

$$U_{\mu\mu}^{\delta_A} = -[I_{\mu}^A + \delta_A \gamma_{\mu\sigma}] - (N_{\mu} - 1)\gamma_{\mu\mu} - \sum_{\nu \neq \mu}^A (N_{\nu} \gamma_{\mu\nu} - K_{\mu\nu}) \quad (8)$$

$\mu$  and  $\nu$  represent only the  $\pi$ -orbitals.

$N_{\mu(\nu)}$  is the number of electrons in the orbital  $\mu(\nu)$ . The first term in Eq. (8) is approximated by the following relations:

$$I_{\mu}^A + \delta_A \gamma_{\mu\sigma} = (1 - \delta_A)I_{\mu}^A + \delta_A I_{\mu}^{A+} \quad \text{for } 0 < \delta_A < 1$$

or

$$= (1 + \delta_A)I_{\mu}^A - \delta_A I_{\mu}^{A-} \quad \text{for } -1 < \delta_A < 0 \quad (9)$$

$I_{\mu}^{A+}$  and  $I_{\mu}^{A-}$  are the corresponding ionization potentials for the  $\sigma$ -cation  $A^+$  and the  $\sigma$ -anion  $A^-$ , respectively [9, 10]. The values for the ionization potentials are given in Table 1. For the determination of  $V_{\mu B}^{\delta_B}$  the definition  $(\mu\mu|B)$  of the penetration integral from Goeppert-Mayer and Sklar [11] is used and it is assumed that  $\gamma_{\mu r} \approx \gamma_{\mu\rho} \approx \gamma_{AB}$  for  $\pi$ -( $\rho$ ) and  $\sigma$ -( $r$ ) orbitals on atom  $B$ . That means the  $\sigma$ -polarization in the  $r$ -orbitals on  $B$  is felt by the electron in the  $\mu$ -orbital on  $A$  in the same way as a  $\pi$ -polarization in  $\rho$ -orbitals on  $B$ . Therefore, the core-charge  $\delta_B$  will be formally distributed among all  $\pi$ -orbitals of  $B$ .

$$V_{\mu B}^{\delta_B} = -(\mu\mu|B) + \sum_{\rho} (N_{\rho} + \delta_B/n_B)\gamma_{\mu\rho} \quad (10)$$

**Table 1.**  $\pi$ -parameter

Atom	Valence configuration	$I_\pi$	$\gamma_{\pi\pi}$	$K_{\pi\pi'}$
N <sup>a</sup>	$tr^1tr^1tr^2\pi^1$	11.4 <sup>1</sup>	12.34 <sup>2</sup>	—
N <sup>+b</sup>	$tr^1tr^1tr^1\pi^1$	27.27 <sup>d</sup>	16.75 <sup>3</sup>	—
C <sup>c</sup>	$tr^1tr^1tr^1\pi^1$	9.84 <sup>4</sup>	10.53 <sup>5</sup>	—
Fe	3d	8.7 <sup>6</sup>	11.33 <sup>7</sup>	0.631 <sup>8</sup>
Fe( $\sigma+$ )		19.5 <sup>9</sup>		

<sup>a</sup> From NH<sub>2</sub>; <sup>b</sup> from NH<sub>3</sub><sup>+</sup>; <sup>c</sup> from CH<sub>3</sub>; <sup>d</sup>  $I_\pi(\text{NH}_3^+) = I_\pi(\text{NH}_3) + \gamma_{\pi\pi}$  [33, 35]  
<sup>1</sup> [33]; <sup>2</sup> [34]; <sup>3</sup> [35]; <sup>4</sup> [36]; <sup>5</sup> [37]; <sup>6</sup> [14]; <sup>7</sup> difference between the first and second ionization potential [19]; <sup>8</sup> from Slater-Condor-Parameters [9]; <sup>9</sup> graphic estimation from the experimental ionization potentials taken from Moore's tables [38]

$n_B$  represents the number of  $\pi$ -orbitals of  $B$ . Considering the Eqs. (4), (8) and (10),  $H_{\mu\mu}^A$  is given by the following Eq. (11):

$$H_{\mu\mu}^A = -[I_\mu^A(\delta_A) + (N_\mu - 1)\gamma_{\mu\mu}] - \sum_{\nu \neq \mu}^A (N_\nu \gamma_{\mu\nu} - K_{\mu\nu}) + \sum_{B \neq A} \left[ (\mu\mu|B) - \sum_{\rho}^B (N_\rho + \delta_B/n_B)\gamma_{\mu\rho} \right] \quad (11)$$

### 2.3. Estimation of the Partial $\sigma$ -core Charge Distribution

The partial  $\sigma$ -core charge distribution in the metal complex is estimated by the solution of a two-dimensional  $\sigma$ -electron eigen value problem in EHT approximation with orbitals  $L$ ,  $M$  assumed to be orthogonal:

$$\begin{bmatrix} (H_{LL} - \varepsilon) & H_{LM} \\ H_{ML} & (H_{MM} - \varepsilon) \end{bmatrix} \begin{bmatrix} C_L \\ C_M \end{bmatrix} = 0 \quad (12)$$

$C_L$  and  $C_M$  are LCAO coefficients.

$H_{LL}$  is the negative ionization potential of the ligand lone-pair orbital.  $H_{MM}$  represents the negative ionization potential of the metal  $d^2sp^3$  hybrid orbital. The resonance integral  $H_{LM}$  is calculated according to the Wolfsberg-Helmholtz-relation [12]:

$$H_{LM} = \frac{1}{2}k_\sigma(H_{LL} + H_{MM})S_{LM} \quad (13)$$

$S_{LM}$  is the overlap integral between the ligand lone-pair orbital and the metal  $d^2sp^3$  hybrid orbital.  $k_\sigma$  is a gauge parameter. As shown below, the value of  $k_\sigma$  has an essential meaning for a correct description of the experimental absorption spectra.

The difference  $(2 - 2C_L^2)$  is the partial charge which is transferred from the ligand lone-pair orbital into the empty metal  $d^2sp^3$  hybrid orbital. The partial

$\sigma$ -core charges  $\delta$  are given in the following relations:

$$\begin{aligned}\delta_{\text{ligand}} &= (2 - 2C_L^2) \\ \delta_{\text{metal}} &= \text{oxidation number} - \sum_L (2 - 2 \cdot C_L^2)\end{aligned}\quad (14)$$

The lone-pair orbital ionization potential  $H_{LL}$  of the nitrogen is taken from Hinze and Jaffé [9].

$$N(tr^1 tr^1 tr^2 \pi^1) \rightarrow N^+(tr^1 tr^1 tr^1 \pi^1) = 15.09 \text{ eV}$$

The ionization potential  $I_{d\sigma}(H_{MM})$  for the iron  $d^2 sp^3$  hybrid orbital  $d\sigma$  is estimated as shown:

$$\begin{aligned}d\sigma &= 1/\sqrt{6} 4s + 1/\sqrt{2} 4p_z + 1/\sqrt{3} 3d_z^2 \\ \gamma_{d\sigma d\sigma} &= \frac{1}{36}\gamma_{ss} + \frac{1}{4}\gamma_{pp} + \frac{1}{9}\gamma_{dd} + \frac{1}{6}\gamma_{sd} + \frac{1}{3}\gamma_{pd} \\ I_{d\sigma} &= \frac{1}{6}I_{4s} + \frac{1}{2}I_{4p} + \frac{1}{3}I_{3d}\end{aligned}$$

The following values are used [13]:

$$\begin{aligned}\gamma_{ss} &= 6.162 \text{ eV}; & \gamma_{pp} &= 5.423 \text{ eV}; & \gamma_{dd} &= 11.33 \text{ eV} [14] \\ \gamma_{sp} &= 6.414 \text{ eV}; & \gamma_{sd} &= 9.509 \text{ eV}; & \gamma_{pd} &= 8.203 \text{ eV} \\ I_{4s} &= 7.9 \text{ eV}; & I_{4p} &= 4.55 \text{ eV}; & I_{3d} &= 8.7 \text{ eV} [14]\end{aligned}$$

Using these values  $I_{d\sigma} = 6.5 \text{ eV}$  is obtained. The electron affinity is calculated according to  $E_{d\sigma} = I_{d\sigma} - \gamma_{d\sigma d\sigma} = -1.15 \text{ eV}$ . The population of the metal orbital  $d^2 sp^3$  yields for  $I_{d\sigma}(\pm 0) = \frac{1}{3}I_{d\sigma} + \frac{2}{3}E_{d\sigma} = 1.4 \text{ eV}$ .  $k_\sigma$  is varied between 1.7 and 2.0.

#### 2.4. Two-Center-One-Electron Integral $H_{\mu\nu}$

$H_{\mu\nu}^A$  is equal zero. For the two-center integral  $H_{\mu\nu}^{A,B}$  which is called resonance integral  $\beta_{\mu\nu}$  a Wolfsberg–Helmholtz relation [12] is used for the metal-ligand interaction:

$$\beta_{\mu\nu} = \frac{1}{2}k_\pi(IP_\mu + IP_\nu)S_{\mu\nu} \quad (15)$$

A value of 1.89 is taken for  $k_\pi$  according to the IEHT calculations by Zerner et al. [7]. In the method presented here the first term in the brackets of Eq. (11) is used for  $IP_{\mu(\nu)}$ . For the other bonds Eq. (16) is used:

$$\beta_{\mu\nu} = \beta_0 S_{\mu\nu}/S(1.4 \text{ \AA}) \quad (\beta_0 = -2.318 \text{ eV} [15]) \quad (16)$$

The Slater exponents used for the calculation of the overlap integrals  $S_{\mu\nu}$  are given in Table 2.

#### 2.5. Two-electron Integrals $\gamma_{\mu\mu}$ , $\gamma_{\mu\rho}$ and $K_{\mu\nu}$

According to Pariser [16]  $\gamma_{\mu\mu}$  is estimated by the difference between the ionization potential and the electron affinity.  $\gamma_{\mu\rho} = \gamma_{AB}$  is calculated using the Mataga–

**Table 2.** Slater exponents [14]

Atom	Orbitals		
	<i>s</i>	<i>p</i>	<i>d</i>
C	1.6083	1.5679	—
N	1.9237	1.9170	—
Fe	1.3700	1.3700	2.7220

Nishimoto approximation [17].  $(2\gamma_{\mu\nu} - K_{\mu\nu})$  is determined by means of Slater-Condon parameters [9].

### 2.6. Penetration Integrals ( $\mu\mu|B$ )

The contribution of the penetration integral to the  $H_{\mu\mu}$  integral of the carbon and nitrogen atoms in the organic ligands is implicitly considered using the ionization potentials of the corresponding hydrogen compounds (CH<sub>3</sub>-radical instead of the C-atom [18]). As shown by Jung and Sauer [19] for the  $sp^2$  carbon atom of benzene 65% of the contribution of the penetration integral to  $H_{\mu\mu}$  can implicitly be obtained using the ionization potential of the methyl radical instead of the valence state ionization potential of the C-atom with  $sp^2$  hybridization.

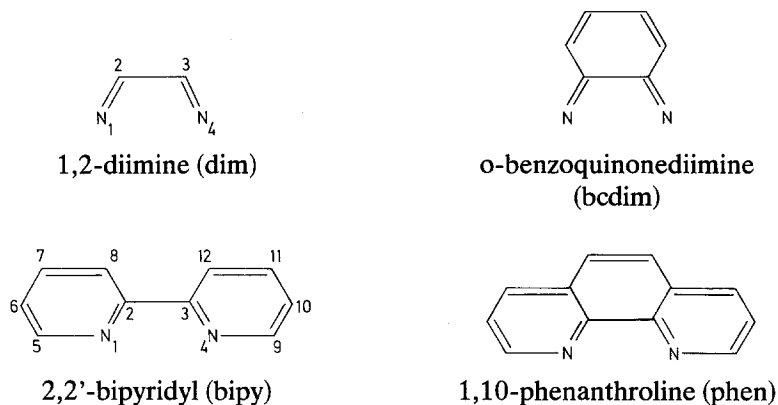
The penetration of the metal atom with the ligand is reduced to the penetration between the metal and the ligand atom directly bound to the metal. The nucleus attraction and two-center coulomb integrals necessary for the estimation of these penetration integrals are calculated according to the method from Todd et al. [20]. A formal population of the six  $d^2sp^3$  hybrid orbitals of the iron atom with  $\frac{1}{3}$  electrons and of the three  $d\pi$  orbitals with 2 electrons was assumed.

### 3. Application of the $\pi$ -INDO-CI Method to Iron(II)-trisdiimine Complexes

The iron(II) trisdiimine complexes seem to be good examples to test the method because of the following arguments. (i) The diimine complexes possess a characteristic absorption band in the visible region ("diimine band") which is experimentally and theoretically clearly determined as charge-transfer transition  $d\pi \rightarrow \pi^*$  (ligand) [21]. The trisdiimine complexes possess a high symmetry ( $D_3$ ). The calculated polarization of the transition can be compared with experimental polarization measurements showing an *E* symmetry for the charge-transfer transition [22, 23].

The energy and intensity of the characteristic CT band strongly depend on the nature of the ligands. Schlosser and Hoyer [24] have shown that diimine complexes with non-heterocyclicly bound nitrogen atoms exhibit a large red-shift of the CT band with increasing number of aromatic rings. Contrarily, the diimine complexes with heterocyclicly bound nitrogen atoms show a small blue-shift or

no shift. This qualitatively different behaviour shall be verified using the  $\pi$ -INDO-CI method. Four trisdiiimine iron(II) complexes (two with non-heterocyclicly and two with heterocyclicly bound nitrogen atoms) are calculated.



The comparison of the calculation with the experiment, therefore, is the first step to test the method.

(ii) There are quantum chemical calculations of trisdiiimine complexes using  $\pi$ -electron methods. A comparison of the results permits conclusions about the suitability of the method. That is the second step of the test presented in the discussion.

For the calculations the following bond distances are used [6].

$$\text{dim: } R_{1,2} = 1.2878 \text{ \AA}; R_{2,3} = 1.46 \text{ \AA}; R_{\text{Fe-N}} = 2.0 \text{ \AA}$$

$$\text{bipy: } R_{1,2} = 1.3394 \text{ \AA}; R_{2,3} = 1.47 \text{ \AA}; R_{1,5} = 1.3394 \text{ \AA};$$

$$R_{5,6} = 1.3958 \text{ \AA}; R_{6,7} = 1.3936 \text{ \AA}; R_{7,8} = 1.3936 \text{ \AA};$$

$$R_{2,8} = 1.3958 \text{ \AA}; R_{\text{Fe-N}} = 2.0 \text{ \AA}$$

bcdim and phen: in analogy to bipy; The remaining bonds are assumed to be 1.4 \AA.

### 3.1. Results for the Calculated Electronic Transitions in Comparison to the Experiment

#### 3.1.1. Diimine complexes with non-heterocyclicly bound nitrogen atoms

Figure 1 shows the dependence of the transition energy of the CT band on the  $k_\sigma$  factor. The transition energy is reduced with enlarged  $k_\sigma$ . The best agreement with the experiment is obtained with  $k_\sigma = 1.966$ . For this value the CT transition, which is in agreement with polarization measurements [22, 23] according to the twofoldly degenerate representation  $E$ , possesses the composition:

$$50\%(\text{HOMO}(E) \rightarrow \text{LUMO}(A_2)) + 47\%(\text{HOMO}(E) \rightarrow \text{LUMO}(E))$$



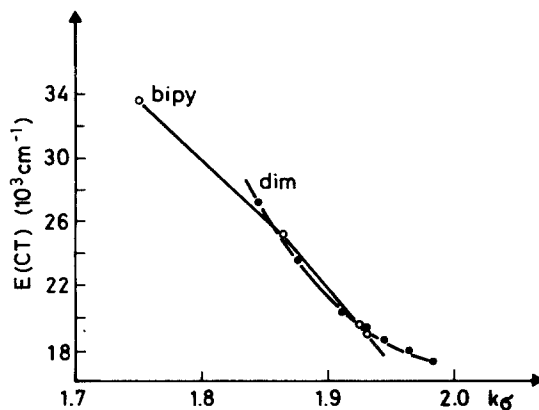


Fig. 1. The calculated energy of the characteristic charge-transfer transition ( $E(CT)$ ) as a function of the value of  $k_\sigma$

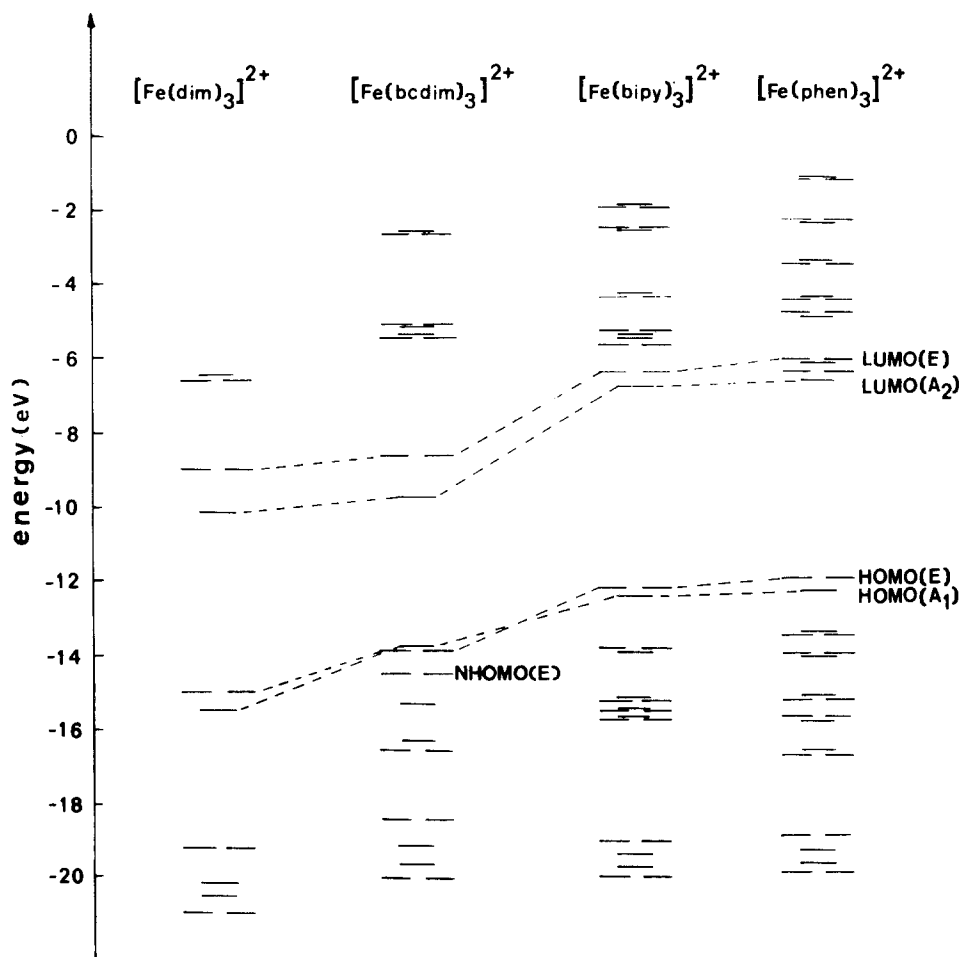


Fig. 2. MO schemes for the calculated trisdiimine iron(II) complexes

**Table 3.** Calculated and experimental [6] electronic transitions of  $[\text{Fe}(\text{dim})_3]^{2+}$ 

Sym.	% CT	Calculation		Experiment [11] <sup>a</sup> $\nu$ (log $\epsilon$ )
		$\nu$ ( $f$ )	$\nu'$ ( $f'$ )	
$A_2$	61.9 (Fe $\rightarrow$ L)	10.84 (0.000)	13.2 (0.01)	—
$A_2$	42.1 (Fe $\rightarrow$ L)	12.19 (0.001)		
$A_2$	83.7 (Fe $\rightarrow$ L)	12.46 (0.002)		
$E$	52.8 (Fe $\rightarrow$ L)	13.45 (0.004)		
$E$	53.1 (Fe $\rightarrow$ L)	18.00 (0.400)		
$A_1$	47.1 (Fe $\rightarrow$ L)	34.24 (0.000)	34.2 (0.00)	—
$E$	76.5 (Fe $\rightarrow$ L)	43.46 (0.048)	43.8 (0.64)	44.3 (4.6)
$E$	68.3 (Fe $\rightarrow$ L)	43.58 (0.021)		
$A_2$	62.4 (Fe $\rightarrow$ L)	43.60 (0.140)		
$A_1$	70.4 (Fe $\rightarrow$ L)	43.65 (0.000)		
$E$	64.2 (Fe $\rightarrow$ L)	43.97 (0.180)		
$A_1$	31.4 (Fe $\rightarrow$ L)	49.92 (0.000)		
$E$	1.8 (Fe $\rightarrow$ L)	50.51 (0.022)		
$A_2$	6.9 (Fe $\rightarrow$ L)	55.23 (0.031)	58.9 (1.11)	54.0 (4.8)
$E$	23.4 (L $\rightarrow$ Fe)	56.22 (0.013)		
$A_2$	16.7 (L $\rightarrow$ Fe)	59.43 (1.005)		
$A_1$	7.2 (L $\rightarrow$ Fe)	59.67 (0.000)		

$\nu$  in  $10^3 \text{ cm}^{-1}$ ;  $\nu'$  = intensity-weighted averaged energy value;  $f$  = oscillator strength (for degenerate transitions the value of only one component is given);  $f'$  = sum of all oscillator strengths of one group of transitions;  $l$  = ligand  $\pi$ -system; Fe =  $d\pi$ -orbitals of the iron

<sup>a</sup> tris(glyoxal-bis-*N*-methylimine)iron(II)iodide in aqueous solution

The molecular orbitals HOMO( $A_1$ ) and HOMO( $E$ ) (Fig. 2) are predominantly  $d\pi$  orbitals (64% and 80%, respectively). LUMO( $A_2$ ) and LUMO( $E$ ) are derived from the LUMO of the free ligands. The  $d\pi$  contribution of LUMO( $E$ ) is 24%. Because of symmetry reasons LUMO( $A_2$ ) does not contain  $d\pi$  admixtures. In Table 3 the calculated transition energies and intensities are compared with the experimental ones [6]. The calculated electronic transitions are collected in several regions presented by intensity-weighted averaged energy values. The first three regions consist of transitions possessing large CT parts (50–84%)<sup>1</sup>. Contrarily, the region around  $58.9 \cdot 10^3 \text{ cm}^{-1}$  contains predominantly intra-ligand transitions with partially large  $\pi$ -charge donation from the ligand to the partially empty  $d\pi$  orbitals.

For the calculation of the bcdim complex it is assumed that the best value of  $k_\sigma$  (1.966) found for the dim complex is valid for tris-complexes of diimine with

<sup>1</sup> For characterization of the electronic transitions as partial charge transfer transitions following definition of the “charge-transfer part” is made:

$$\text{CT}(\%) = 100 \sum_{\mu} (P_{\mu\mu} - P_{\mu\mu}^{\text{CI}})$$

$P_{\mu\mu}$  and  $P_{\mu\mu}^{\text{CI}}$  are the electronic densities of the metal orbitals in the electronic ground and excited states, respectively.

**Table 4.** Calculated and experimental [25] electronic transitions of  $[\text{Fe}(\text{bcdim})_3]^{2+}$ 

Sym.	% CT	Calculation		Experiment [25] $\nu(\log \epsilon)$
		$\nu (f)$	$\nu' (f')$	
<i>E</i>	39.0 (Fe → <i>L</i> )	8.31 (0.001)	10.1 (0.09)	—
<i>A</i> <sub>2</sub>	47.4 (Fe → <i>L</i> )	8.47 (0.024)		
<i>A</i> <sub>2</sub>	24.7 (Fe → <i>L</i> )	10.40 (0.009)		
<i>E</i>	30.1 (Fe → <i>L</i> )	10.80 (0.030)	14.4 (0.32)	14.26 (4.26) $\nu(0-0)$
<i>E</i>	10.1 (Fe → <i>L</i> )	14.45 (0.320)		
<i>E</i>	33.1 (Fe → <i>L</i> )	15.46 (0.470)	15.5 (0.47)	s15.50 (4.20) $\nu(0-1)$
<i>A</i> <sub>2</sub>	17.9 (Fe → <i>L</i> )	17.55 (0.065)	22.3 (0.19)	23.40 (3.32)
<i>E</i>	21.4 (Fe → <i>L</i> )	24.62 (0.033)		
<i>A</i> <sub>1</sub>	25.1 ( <i>L</i> → Fe)	24.95 (0.000)		
<i>A</i> <sub>2</sub>	14.3 ( <i>L</i> → Fe)	25.18 (0.056)	33.9 (0.02)	s34.50 (3.43)
<i>E</i>	22.4 ( <i>L</i> → Fe)	27.75 (0.052)		
<i>A</i> <sub>1</sub>	2.9 ( <i>L</i> → Fe)	32.58 (0.000)	40.9 (1.56)	43.50 (4.40)
<i>E</i>	0.9 (Fe → <i>L</i> )	33.92 (0.015)		
<i>A</i> <sub>1</sub>	10.9 (Fe → <i>L</i> )	35.23 (0.000)		
<i>E</i>	7.6 (Fe → <i>L</i> )	40.06 (0.517)	40.9 (1.56)	43.50 (4.40)
<i>E</i>	17.3 ( <i>L</i> → Fe)	42.42 (0.228)		
<i>A</i> <sub>1</sub>	5.9 ( <i>L</i> → Fe)	44.06 (0.000)		
<i>E</i>	21.4 ( <i>L</i> → Fe)	44.38 (0.020)	45.01 (0.008)	45.22 (0.000)
<i>A</i> <sub>2</sub>	9.0 ( <i>L</i> → Fe)	44.70 (0.010)		
<i>E</i>	30.5 (Fe → <i>L</i> )	45.01 (0.008)		
<i>A</i> <sub>2</sub>	16.9 (Fe → <i>L</i> )	45.22 (0.000)	45.68 (0.000)	
<i>A</i> <sub>1</sub>	35.3 (Fe → <i>L</i> )	45.68 (0.000)		

$\nu$  in  $10^3 \text{ cm}^{-1}$ ; denotations as in Table 3; s = shoulder; CI calculation with the 75 lowest configurations.

non-heterocyclicly bound nitrogen atoms, that means for the bcdim complex, too. In Table 4 the results of the calculation are presented. The experimentally observed red-shift of the CT transition ( $\text{CT}_1$ ) with an enlargement of the  $\pi$ -system due to one aromatic ring [25] is correctly verified by the calculation. The experimental and calculated red-shift are  $3.8 \cdot 10^3 \text{ cm}^{-1}$  and  $3.6 \cdot 10^3 \text{ cm}^{-1}$ , respectively. This strong red-shift, however, is accompanied by a strong decrease of the CT part of the CT band from 53% to 10%. Furthermore, a new CT transition ( $\text{CT}_2$ ) appears in the visible region possessing a CT part of 30%. A strong configuration interaction between both CT transitions exists:

$$\begin{aligned} \text{CT}_1(14.45 \cdot 10^3 \text{ cm}^{-1}) &= 31\%(\text{HOMO}(E) \rightarrow \text{LUMO}(A_2)) \\ &+ 5\%(\text{HOMO}(E) \rightarrow \text{LUMO}(E)) \\ &+ 23\%(\text{NHOMO}(E) \rightarrow \text{LUMO}(A_2)) \\ &+ 23\%(\text{NHOMO}(E) \rightarrow \text{LUMO}(E)) \end{aligned}$$

$$\begin{aligned} \text{CT}_2(15.46 \cdot 10^3 \text{ cm}^{-1}) &= 11\%(\text{HOMO}(E) \rightarrow \text{LUMO}(A_2)) \\ &+ 20\%(\text{HOMO}(E) \rightarrow \text{LUMO}(E)) \\ &+ 60\%(\text{NHOMO}(E) \rightarrow \text{LUMO}(A_2)) \\ &+ 0.1\%(\text{HNOMO}(E) \rightarrow \text{LUMO}(E)) \end{aligned}$$

The  $d\pi$  orbitals contribute in NHOMO( $E$ ), HOMO( $E$ ), HOMO( $A_1$ ) and LUMO( $E$ ) with 22%, 30%, 25% and 29%, respectively.

### 3.1.2. Diimine complexes with heterocyclic bound nitrogen atoms

For the  $[\text{Fe}(\text{bipy})_3]^{2+}$  complex the variation of  $k_\sigma$  qualitatively yields the same alterations in the energy of the CT band (Fig. 1) in comparison with the  $[\text{Fe}(\text{dim})_3]^{2+}$  complex. The best agreement between the calculation and the experiment is obtained for  $k_\sigma = 1.925$  (Table 5). The CI composition of the CT

**Table 5.** Calculated and experimental [6, 26] electronic transitions of  $[\text{Fe}(\text{bipy})_3]^{2+}$

Sym.	% CT	Experiment			
		Calculation $\nu$ ( $f$ )	$\nu'$ ( $f'$ )	[6]* $\nu$ (log $\epsilon$ )	[26]** $\nu$ ( $f'$ )
$A_2$	66.3 (Fe $\rightarrow$ L)	18.04 (0.005)	18.1 (0.01)	s20.5 (3.80)	19.1 } ( $\nu(0-1)$ ) (0.148)
$E$	70.5 (Fe $\rightarrow$ L)	18.24 (0.001)			
$E$	70.2 (Fe $\rightarrow$ L)	19.20 (0.000)			
$E$	69.9 (Fe $\rightarrow$ L)	19.30 (0.253)	19.3 (0.51)	s20.5 (3.80)	20.4 } ( $\nu(0-1)$ )
$A_2$	79.8 (Fe $\rightarrow$ L)	19.30 (0.002)			
$A_1$	71.2 (Fe $\rightarrow$ L)	24.62 (0.000)	24.6 (0.00)	s25.5 (3.45)	25.6 } (0.135)
$E$	70.8 (Fe $\rightarrow$ L)	28.81 (0.004)			
$A_2$	67.7 (Fe $\rightarrow$ L)	28.83 (0.093)	29.5 (0.62)	s28.6 (3.75)	28.7 } (0.135)
$E$	71.9 (Fe $\rightarrow$ L)	29.34 (0.151)			
$A_1$	75.2 (Fe $\rightarrow$ L)	29.73 (0.000)			
$E$	80.3 (Fe $\rightarrow$ L)	29.84 (0.114)	33.4 (4.77)	s34.5 (4.72)	33.6 } (0.832)
$E$	45.6 (Fe $\rightarrow$ L)	32.15 (0.084)			
$A_2$	60.5 (Fe $\rightarrow$ L)	32.39 (0.109)	35.5 (3.45)	s34.5 (4.72)	34.5 } (0.832)
$A_1$	74.5 (Fe $\rightarrow$ L)	32.45 (0.000)			
$E$	73.1 (Fe $\rightarrow$ L)	32.53 (0.002)			
$E$	69.5 (Fe $\rightarrow$ L)	33.91 (0.047)	43.2 (1.53)	s38.6 (4.22)	38.8 } (0.459)
$A_2$	76.1 (Fe $\rightarrow$ L)	33.95 (0.030)			
$E$	40.3 (Fe $\rightarrow$ L)	34.81 (0.393)	46.3 (0.10)	s42.0 (4.36)	41.5 } (0.459)
$A_2$	22.6 (Fe $\rightarrow$ L)	36.22 (2.262)			
$E$	5.1 ( $L \rightarrow$ Fe)	40.27 (0.016)			
$A_2$	5.2 ( $L \rightarrow$ Fe)	40.35 (0.128)	43.2 (1.53)	s38.6 (4.22)	38.8 } (0.459)
$A_1$	2.6 ( $L \rightarrow$ Fe)	41.06 (0.000)			
$E$	6.0 ( $L \rightarrow$ Fe)	41.24 (0.090)	46.3 (0.10)	s42.0 (4.36)	41.5 } (0.459)
$A_1$	20.8 (Fe $\rightarrow$ L)	43.37 (0.000)			
$A_1$	14.5 (Fe $\rightarrow$ L)	43.61 (0.000)			
$E$	2.5 ( $L \rightarrow$ Fe)	43.91 (0.592)	46.3 (0.10)	s42.0 (4.36)	41.5 } (0.459)
$E$	1.3 (Fe $\rightarrow$ L)	45.06 (0.000)			
$A_2$	2.0 (Fe $\rightarrow$ L)	45.53 (0.001)	46.3 (0.10)	s42.0 (4.36)	41.5 } (0.459)
$E$	2.2 ( $L \rightarrow$ Fe)	46.12 (0.043)			
$A_1$	23.4 (Fe $\rightarrow$ L)	48.10 (0.000)			
$A_2$	1.5 (Fe $\rightarrow$ L)	48.23 (0.002)	46.3 (0.10)	s42.0 (4.36)	41.5 } (0.459)
$E$	1.2 ( $L \rightarrow$ Fe)	48.31 (0.003)			

$\nu$  in  $10^3 \text{ cm}^{-1}$ ; denotations as in Table 3; s = shoulder; CI calculation with the lowest 75 configurations.

\*  $\text{Fe}(\text{bipy})_3 \cdot \text{SO}_4 \cdot 5 \text{H}_2\text{O}$  in methanol

\*\*  $\text{Fe}(\text{bipy})_3 \cdot \text{Cl}_2 \cdot 7 \text{H}_2\text{O}$  in aqueous solution

transition in the visible region is:

$$55\%(\text{HOMO}(E) \rightarrow \text{LUMO}(A_2)) + 41\%(\text{HOMO}(E) \rightarrow \text{LUMO}(E))$$

The  $d\pi$  orbitals are localized in  $\text{HOMO}(E)$ ,  $\text{HOMO}(A_1)$  and  $\text{LUMO}(E)$  to 75%, 81% and 16%, respectively. The calculated ratio of the oscillator strengths of the different groups of electronic transitions (Table 5) is in good agreement with the experimental one:

second : third : fourth : fifth group of transitions

0.15 : 0.18 : 1 : 0.44 for the calculation

0.18 : 0.16 : 1 : 0.55 for the experiment [26]

For the calculation of the  $[\text{Fe}(\text{phen})_3]^{2+}$  complex the same  $k_\sigma$  (1.925) as for the  $[\text{Fe}(\text{bipy})_3]^{2+}$  complex is used. Table 6 summarizes the results. In agreement with the experiment [27] the characteristic CT transition in the visible region has approximately the same energy as obtained for the bipy complex. The CI

**Table 6.** Calculated and experimental [27] electronic transitions of  $[\text{Fe}(\text{phen})_3]^{2+}$

Sym.	% CT	Calculation		Experiment [27] $\nu$ (log $\epsilon$ )
		$\nu$ ( $f$ )	$\nu'$ ( $f'$ )	
$A_2$	66.1 (Fe $\rightarrow$ L)	18.07 (0.008)	18.2 (0.01)	—
$E$	70.1 (Fe $\rightarrow$ L)	18.63 (0.001)		
$E$	67.9 (Fe $\rightarrow$ L)	19.17 (0.257)	19.2 (0.53)	19.60 (4.05) $\nu(0-0)$
$E$	71.4 (Fe $\rightarrow$ L)	19.47 (0.008)		
$A_2$	80.8 (Fe $\rightarrow$ L)	19.59 (0.004)		
$A_1$	69.8 (Fe $\rightarrow$ L)	22.25 (0.000)	22.3 (0.00)	—
$E$	71.9 (Fe $\rightarrow$ L)	23.88 (0.026)	24.4 (0.77)	22.99 (3.85)
$E$	71.8 (Fe $\rightarrow$ L)	24.12 (0.131)		
$A_2$	72.2 (Fe $\rightarrow$ L)	24.16 (0.243)		
$A_1$	75.1 (Fe $\rightarrow$ L)	24.76 (0.000)		
$E$	80.5 (Fe $\rightarrow$ L)	25.08 (0.106)		
$A_1$	9.7 (Fe $\rightarrow$ L)	31.36 (0.000)	32.4 (0.60)	31.21 (3.55)
$E$	9.0 (Fe $\rightarrow$ L)	31.57 (0.046)		
$E$	2.5 (Fe $\rightarrow$ L)	32.50 (0.099)		
$A_2$	2.2 (Fe $\rightarrow$ L)	32.65 (0.307)		
$A_1$	51.9 (Fe $\rightarrow$ L)	33.94 (0.000)	37.6 (1.11)	37.59 (4.95)
$E$	55.9 (Fe $\rightarrow$ L)	35.17 (0.016)		
$A_2$	62.6 (Fe $\rightarrow$ L)	35.71 (0.027)		
$E$	58.7 (Fe $\rightarrow$ L)	35.83 (0.018)		
$A_2$	72.6 (Fe $\rightarrow$ L)	36.90 (0.022)		
$E$	8.7 (Fe $\rightarrow$ L)	37.54 (0.383)		
$A_1$	18.7 (Fe $\rightarrow$ L)	37.99 (0.000)		
$E$	1.0 (L $\rightarrow$ Fe)	38.69 (0.115)	—	44.36 (4.91)

$\nu$  in  $10^3 \text{ cm}^{-1}$ ; denotations as in Table 3;  $s$  = shoulder; CI calculations with the lowest 74 configurations.

\*  $[\text{Fe}(\text{phen})_3] - \text{Cl}_2 \cdot 7 \text{ H}_2\text{O}$  in aqueous solution.

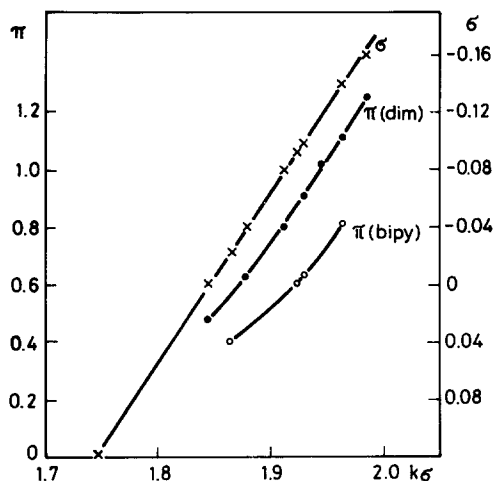


**Fig. 3.** The  $\sigma$  and the  $\pi$  charges of the iron center for the complexes  $[\text{Fe}(\text{dim})_3]^{2+}$  and  $[\text{Fe}(\text{bipy})_3]^{2+}$  as a function of the value of  $k_\sigma$ .  $\sigma$  represents the ligand- $\sigma$ -donation.  $\pi$  results from the iron- $\pi$ -backdonation

composition is:

$$63\%(\text{HOMO}(E) \rightarrow \text{LUMO}(A_2)) + 26\%(\text{HOMO}(E) \rightarrow \text{LUMO}(E))$$

The  $d\pi$  orbitals are localized in HOMO( $E$ ), HOMO( $A_1$ ) and LUMO( $E$ ) to 67%, 81% and 9%, respectively.

### 3.2. Results for the Electronic Ground State

The variation of  $k_\sigma$  causes variation of the  $\sigma$ -charge at the iron atom. An increasing  $k_\sigma$  value induces an increasing charge which is denoted from the ligand lone-pair orbitals to the empty  $d^2sp^3$  hybrid orbitals of the iron (ligand- $\sigma$ -donation). However, the stronger the ligand- $\sigma$ -donation the stronger the iron- $\pi$ -backdonation as demonstrated in Fig. 3. For the four complexes investigated the  $\sigma$ -,  $\pi$ - and net-charges of the iron atom are shown in Table 7. In the dim and bcdim complex the iron possesses a net charge of about 1. For the bipy and the phen complex, however, the net charge is about 0.5. For all complexes a decrease of the CN- $\pi$ -bond order is obtained compared with that of the free ligands (Table 8). This result agrees with IR measurements [28] showing a decrease of the IR stretch vibration frequency of the CN bond due to the complexation to the iron. Using the relation between the  $\pi$ -bond order and CN

**Table 7.**  $\sigma$ -,  $\pi$ - and net charges

	$k_\sigma = 1.966$		$k_\sigma = 1.925$	
	dim	bcdim	bipy	phen
$\sigma$	-0.140	-0.140	-0.094	-0.094
$\pi$	1.113	1.253	0.603	0.603
net	0.973	1.113	0.509	0.509

**Table 8.** Calculated CN- $\pi$ -bond orders and estimated IR stretch vibration frequencies for the CN bond according to Bayer [28] ( $\nu$  in  $\text{cm}^{-1}$ )

Ligand	$\pi$ -bond order		$\nu$ IR-stretch vibration	
	free	complex	free	complex
dim	0.951	0.776	1650 exp. 1650	1564 exp. 1530
bcdim	0.862	0.658	1621	1514
bipy	0.643	0.547	1507	1443
phen	0.608	0.513	1486	1414

IR-stretch vibration frequency according to Bayer [28] the expected IR frequency can be estimated for the four investigated complexes. Table 8 summarizes the results and shows a good agreement with the experiment for the dim complex the only one for which IR measurements were carried out.

#### 4. Discussion

The calculations according to the  $\pi$ -INDO-CI method yield good qualitative as well as quantitative results for the diimine complexes. The great importance of the relation between the ligand- $\sigma$ -donation and iron- $\pi$ -backdonation for understanding of the absorption spectra of this group of iron complexes is clearly demonstrated by this method. For diimine complexes with heterocyclicly as well as non-heterocyclicly bound nitrogen atoms it is shown that increased ligand- $\sigma$ -donation induces increased iron- $\pi$ -backdonation reflected in a red-shift of the characteristic CT band in the visible region. For a fixed  $k_\sigma$ -value (1.966 and 1.925, respectively) the enlargement of the ligand- $\pi$ -system by one aromatic ring causes a stronger iron- $\pi$ -backdonation only for the diimine complexes with non-heterocyclicly bound nitrogen atoms. This stronger iron- $\pi$ -backdonation in the bcdim complex in comparison with the dim complex is connected with the red-shift of the CT band. Contrarily, no increased iron- $\pi$ -backdonation of the phen complex in comparison with the bipy complex is obtained which reflects in a lack of a red-shift of the CT band. By means of these results the experimentally observed [24] different spectral behaviour of diimine complexes with heterocyclicly and non-heterocyclicly bound nitrogen atoms due to enlargement of the ligand- $\pi$ -system by one aromatic ring may be explained.

The necessity to use different "best"  $k_\sigma$ -values for the two types of diimine complexes originates from the difference between their lone-pair ionization potentials (bipy: 10 eV, molecules with the dim structure: 9.5 eV [19]). Due to the use of atomic lone-pair ionization potential this difference is neglected. However, it can be shown by the solution for  $C_L$  in Eq. (12), the increase of the lone-pair ionization potential with fixed  $k_\sigma$  value is equivalent to a decrease of the  $k_\sigma$  value with fixed lone-pair ionization potential. Therefore, the different  $k_\sigma$  values for the two types of diimine complexes compensate the neglected difference between the lone-pair ionization potentials.

Concerning the origin of the characteristic "diimine" band in the visible region as charge-transfer transition our results are similar to those obtained by Hanazaki et al. [2, 26, 27, 30], Sanders and Day [3, 31, 32] and Blomquist et al. [6].

Although Hanazaki's as well as Sander's calculations verify well the experiment using special gauge values for each complex and show the essential meaning of the metal charge for a correct calculation of the energy of the charge-transfer transition, the  $\pi$ -INDO-CI method presented here gives a more systematic procedure to consider the  $\sigma$ -polarization in the  $\pi$ -calculation. Furthermore, this method reveals the closed relation between ligand- $\sigma$ -donation and metal- $\pi$ -backdonation. The PEEL calculations by Blomquist et al. [6] do not give good results for the electronic transitions. The energy of the CT band is calculated 1900  $\text{cm}^{-1}$  too high (calculated:  $19.9 \times 10^3 \text{ cm}^{-1}$ ; experiment:  $18 \cdot 10^3 \text{ cm}^{-1}$  [6]) for the dim complex, however 3300  $\text{cm}^{-1}$  too low (calculated:  $15.9 \times 10^3 \text{ cm}^{-1}$ ; experiment:  $19.2 \cdot 10^3 \text{ cm}^{-1}$  [6]) for the bipy complex. Therefore, these calculations yield a strong red-shift of the CT band for the bipy complex in comparison with the dim complex. This is, however, in contrast to the experiment. It seems that the explicit consideration of iron valence orbitals  $4s$ ,  $4p$  and  $3d$  and of the ligand lone-pair orbitals in the SCF calculation is not essential for a correct description of the electronic absorption spectra of iron(II) trisdiimine complexes.

*Acknowledgement.* We are grateful to Dr. Benedix and Dr. Birner from the Karl Marx-University Leipzig, GDR, for the calculation of the nucleus attraction and electron interaction integrals.

## References

1. Schläfer, H. L., Gliemann, G.: Einführung in die Ligandenfeldtheorie, Leipzig: Akademische Verlagsgesellschaft Geest & Portig, K.-G., 1967
2. Hanazaki, I., Hanazaki, F., Nagakura, S.: J. Chem. Phys. **50**, 265 (1969)
3. Sanders, N.: J. Chem. Soc. Dalton Trans. 345 (1972)
4. Roos, B.: Acta Chem. Scand. **20**, 1673 (1966).
5. Mayoh, B., Day, P.: Theoret. Chim. Acta (Berl.) **49**, 259 (1978)
6. Blomquist, J., Norden, B., Sundbom, M.: Theoret. Chim. Acta (Berl.) **28**, 313 (1973)
7. Zerner, M., Gouterman, M., Kobayashi, H.: Theoret. Chim. Acta (Berl.) **6**, 363 (1966)
8. Pople, J. A., Beveridge, D. L.: Approximate molecular orbital theory. New York: McGraw-Hill, 1970
9. Hinze, J., Jaffé, H. H.: J. Chem. Phys. **38**, 1834 (1963)
10. Moore, C. E.: Circular of the National Bureau of Standards 467, Washington, 1952
11. Goepfert-Mayer, M., Sklar, A. L.: J. Chem. Phys. **6**, 645 (1938)
12. Wolfsberg, M., Helmholz, L.: J. Chem. Phys. **20**, 837 (1952)
13. Tatsumi, K., Fueno, T.: Bull. Chem. Soc. Japan **49**, 929 (1976).
14. Zerner, M., Gouterman, M.: Theoret. Chim. Acta (Berl.) **4**, 44 (1966)
15. Zahradnik, R., Čársky, P.: J. Chem. Phys. **74**, 1235 (1970)
16. Pariser, R.: J. Chem. Phys. **21**, 568 (1953)
17. Mataga, N., Nishimoto, K.: Z. phys. Chem. (Frankf.) **13**, 140 (1957)
18. Kwiatkowski, S.: Acta Phys. Polonia **29**, 477 (1966)
19. Jung, Ch., Sauer, J.: Doctoral Thesis, Humboldt-University, Berlin, GDR 1975
20. Todd, H. D., Kay, K. G., Silverstone, H. J.: J. Chem. Phys. **53**, 3951 (1970)
21. Krumholz, P.: Structure and Bonding **9**, 139 (1971)



22. Palmer, R. A., Piper, T. S.: *Inorg. Chem.* **5**, 864 (1966)
23. Decurtins, S., Felix, F., Ferguson, J., Gudel, H. U., Ludi, A.: *J. Am. Chem. Soc.* **102**, 4102 (1980)
24. Schlosser, K., Hoyer, E.: *J. Inorg. Nucl. Chem.* **33**, 4370 (1971)
25. Warren, L. F.: *Inorg. Chem.* **16**, 2814 (1977)
26. Hanazaki, I., Nagakura, S.: *Inorg. Chem.* **8**, 648 (1969)
27. Ito, T., Tanaka, N., Hanazaki, I., Nagakura, S.: *Bull. Chem. Soc. Japan* **42**, 702 (1969)
28. Bayer, E., Häfelinger, G.: *Chem. Ber.* **99**, 1689 (1961)
29. tom Dieck, H., Franz, K.-D., Hohmann, F.: *Chem. Ber.* **108**, 163 (1975)
30. Ito, T., Tanaka, N., Hanazaki, I., Nagakura, S.: *Bull. Chem. Soc. Japan* **41**, 365 (1968)
31. Sanders, N., Day, P.: *J. Chem. Soc. (A)* 1190 (1970)
32. Sanders, N.: *J. Chem. Soc. (A)* 1563 (1971)
33. Filesov, F. T.: *Usp. Fiz. Nauk* **81**, 716 (1963)
34. Hinze, J., Whitehead, M. A., Jaffé, H. H.: *J. Am. Chem. Soc.* **84** 540 (1962)
35. Hinze, J., Jaffé, H. H.: *J. Phys. Chem.* **67**, 1501 (1963)
36. Wedenejew, W. J., Guravitsch, L. W., Kondratjew, W. H., Medwedew, W. A., Frankewitsch, E. L.: *Energien chemischer Bindungen, Ionisationspotentiale und Elektronenaffinitäten*, Leipzig, VEB Deutscher Verlag für Grundstoffindustrie, 1971
37. Pilcher, G., Skinner, H. A.: *J. Inorg. Nucl. Chem.* **24**, 937 (1962)
38. Moore, C. R.: *Circular of the National Bureau of Standards*, 467, Washington 1952

Received January 25, 1982